Int J Clin Exp Med 2017;10(3):5622-5628
www.ijcem.com /ISSN:1940-5901/IJCEM0044163

Original Article

Nd: YAG surgical laser effects in canine prostate tissue: ablation effect and damage distribution

Ren Wang[1], Xing Wu[1], Jin-Jin Chen[2], Bing Hu[1]

[1]Department of Ultrasound in Medicine, Shanghai Jiao Tong University Affiliated Sixth People's Hospital, Shanghai Institute of Ultrasound in Medicine, Shanghai 200233, China; [2]Department of Children Care and Health, Shanghai Children's Hospital Affiliated to Shanghai Jiao Tong University, Shanghai 200040, China

Received August 7, 2016; Accepted December 13, 2016; Epub March 15, 2017; Published March 30, 2017

Abstract: Objective: To evaluate therapy effects and capability to preserve adjacent tissues of bilateral focal prostate ablation using Nd: YAG laser a canine model. Methods: 24 male Beagle dogs aged 3.9-7.4 years and weighting 9.4-12.1 kg were used in this study. The dogs underwent single focal Nd: YAG ablation. Applied the reasonable prostatic ablation parameters screened in the study and set different intervals test of fiber lasers for ablation of prostate-urethral tissue, then observed whether thermal damage occurred and therapy effect. Results: the single focal ablation zone area was 0.7 cm^2 but when Distance of double needle laser was 3 mm, the ablation area was 1.25 cm^2. With the distance increased, the ablation area significantly extended. The ablation area was 1.53, 1.62, 1.65 cm^2 when focal distance was 6, 9, 12 mm, respectively. Although the area extended to 1.65 cm^2 when the distance enlarged from 9 cm to 12 cm, the extension range was negligible. Hence, the rational focal distance was 9 mm. In the two-dimensional ultrasonographic examinations, the coagulation necrosis of ablation area showed the approximate oval area with no contrast agent and strong comparison with the surrounding prostate tissue in which enhancement effect of the contract agent exist, which made their boundary more distinct. Conclusion: Nd: YAG prostate ablation is shown to be a safe non-thermal ablative technique capable of preserving the adjacent structures and physiological functions. Further studies are needed to fully explore the advantages of Nd: YAG compared with other ablative techniques.

Keywords: Prostate, Nd: YAG, ablation, technology

Introduction

Benign prostatic hyperplasia (BPH), the noncancerous enlargement of the prostate gland, is one of the most common disorders in aging men. Microscopic evidence of BPH is present in greater than 50% of men by the age of 60 years and in nearly 90% of men by the age of 85 years, with approximately one-fourth of these patients having symptoms during their lifetime that require treatment [1]. Demographic trends in the United States indicate an aging population in which the rate of prostatectomies would be expected to increase [2]. The recent introduction of nonsurgical and minimally invasive options for treatment of symptoms is anticipated to affect this prediction by increasing the number of patients seeking treatment from among the eligible population by 15%-70% [3]. However, less than half of this greater patient population seeking treatment is anticipated to undergo prostatectomy, with the remainder selecting between an increasing number of less invasive or medical methods of management.

Destruction of prostate tissue by exposure to laser energy is a less invasive treatment method that also may have an impact on the number of prostatectomies performed. Advances in optical fiber construction have improved techniques to deliver light efficiently for treatment of the prostate [4]. Preliminary dosimetry reports of free-beam (noncontact) laser effects in canine prostate tissue [5] supported renewed efforts for laser treatment of BPH [6, 7]. The wavelength of the Nd: YAG laser, one of the most commonly available surgical lasers, is poorly absorbed by tissue proteins and allows propagation of thermal energy, which results in coagulative necrosis [8, 9]. This characteristic is desirable for treating the larger tissue volumes of BPH, although most surgeons are

Table 1. Influence of different single focus laser time and power on canine prostate ablation

	Group A			Group B		
	3 w 5 min	5 w 5 min	7 w 5 min	5 w 3 min	5 w 5 min	5 w 7 min
Prostate zone size (ml)	4.32±0.62	6.83±0.34*	6.35±0.25*	5.11±0.52	6.83±0.34#	6.63±0.29#

*P<0.05, compared with Group 3 w 5 min. #P<0.05, compared with Group 5 w 3 min.

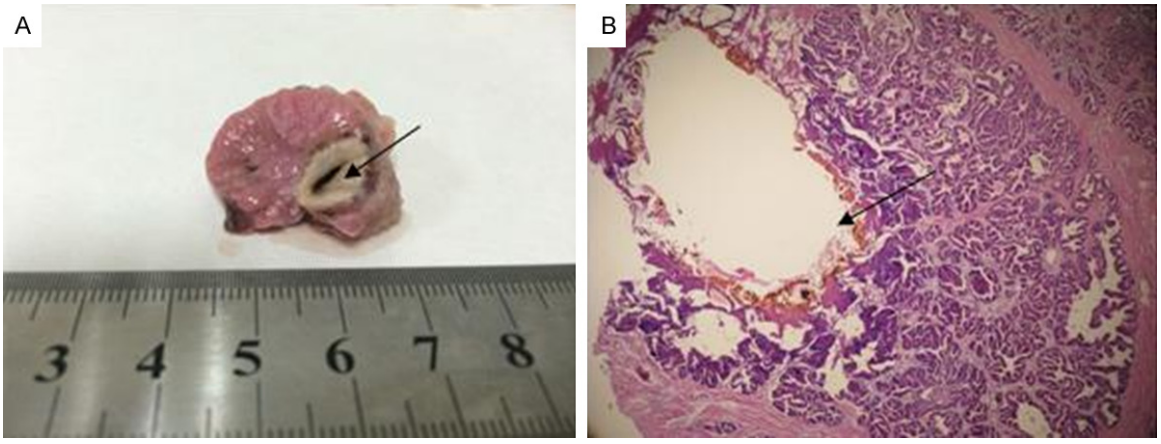

Figure 1. Canine prostate histopathologic examination after single focal Nd: YAG. A: Represents TTC staining of prostate gross cross-sectional slices where there was the narrow annular hyperemia edema zone of dark red band surrounding ablation zone and that four regions existed in outward area hyperemia from the center to the margin which was the vaporizing cavity Area, brown carbonized area, dark necrotic area and inflammatory edema area in sequence. B: Represents-focal ablation of prostate after HE staining under pathological expression (*200) which included visible melting stove from the central cavity to bleeding peripheral congestion.

understandably reluctant to apply this energy near adjacent structures such as the urinary sphincter or bladder neck, where damage is undesirable [10, 11]. In the present study, we sought to evaluate erectile function, side-effects and preservation of adjacent tissues after a bilateral focal prostate ablation.

Materials and methods

Imaging evaluation of combination of different power and time of single fiber laser ablation canine prostate

24 male Beagle dogs aged 3.9-7.4 years and weighting 9.4-12.1 kg were used in this study [13, 14]. The dogs underwent single focal LE-DC ablation by the monopolar electrode Nano-Knife device. The dogs were equally assigned to two groups for final pathological evaluation at 7 days after ablation. The relevant parameters were shown as follow:

Group A: 3 w 5 min, 5 w 5 min, 7 w 5 min.

Group B: 5 w 3 min, 5 w 5 min, 5 w 7 min.

After ablation, the ultrasonic imaging was conducted and prostate focal ablation zone sizes were measured. Then, pathologic specimens of the biggest ablation zone size were collected, then the depth and width of thermal coagulation damage were measured macroscopically. Lesion volume was estimated by assuming a half ellipsoid: volume $=\pi/6*$ (depth) $(\text{width})^2$. HE dyeing was applied for evaluating urothelium change and urethra and prostate boundary situation followed by measuring and comparing the changes of the single fiber ablation zone size between the adjacent urethra prostate and inner prostate organization.

Combination of two bilateral focus laser-melting experiment

According to the reasonable prostatic ablation parameters of energy power and explore time screened in first part, we set a serial interval distance of bare-end bilateral fibers for ablation of prostate-urethral tissue adjacent to melt, then observed whether thermal damage occurred [15]. 24 male Beagle dogs aged 3.9-7.4 years and weighting 9.4-12.1 kg were used in the bilateral focus laser melting experiment.

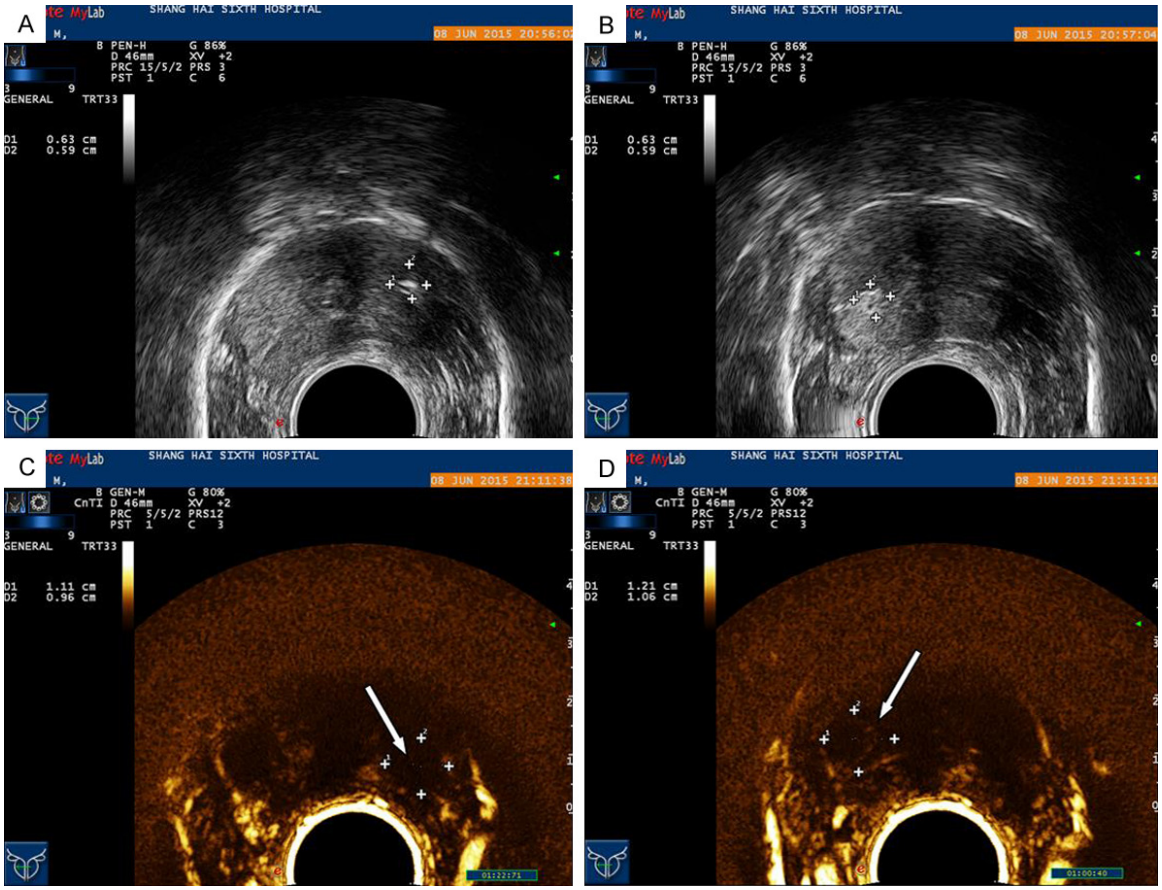

Figure 2. Two-dimensional ultrasonographic examinations of single focus laser ablation. A: Represents ultrasonographic examination in the frontage of tissue section before ablation. B: Represents ultrasonographic examination in the back of tissue section before ablation. C: Represents ultrasonographic examination in the frontage of tissue section after ablation and there was remarkable micro-bubble in the laser ablation area which was absence of the contract agent, but the surrounding normal prostate tissue filling contrast agent showed clear echogenicity in CEUS examination after 5 min ablation. D: Represents ultrasonographic examination in the back of tissue section after ablation. There was also remarkable micro-bubble in the laser ablation area.

Table 2. Relation of focal distance and ablation zone area

Focal distance (mm)	Ablation zone area (cm^3)
0	0.7[a]
3	1.25
6	1.53*
9	1.62*
12	1.65*

[a]single focal lase ablation. *P<0.05, compared with Group focal distance of 3 mm.

After 5 min ablation, the ultrasonic imaging or MRI enhancement were implemented followed observation of the melting focal zone, measurement of its size. Eventually, pathologic specimens were collected, and HE dyeing was conducted.

At termination, a comprehensive necropsy was performed to evaluate for potential injury to adjacent tissues, that is prostate, bladder, ureters, urethra as well as rectal wall. Specific attention was devoted to microscopic examination of the prostatic capsule, urethra, nervous tissues and rectal wall. The study protocol was reviewed and approved by the Institutional Animal Care and Use Committee and carried out under Good Laboratory Practice conditions.

Statistics

Statistically derived experimental results are given as means ± SD. Curve fits of the experimental results were made using the mean values. Differences in results between depths were tested for significance using the Student

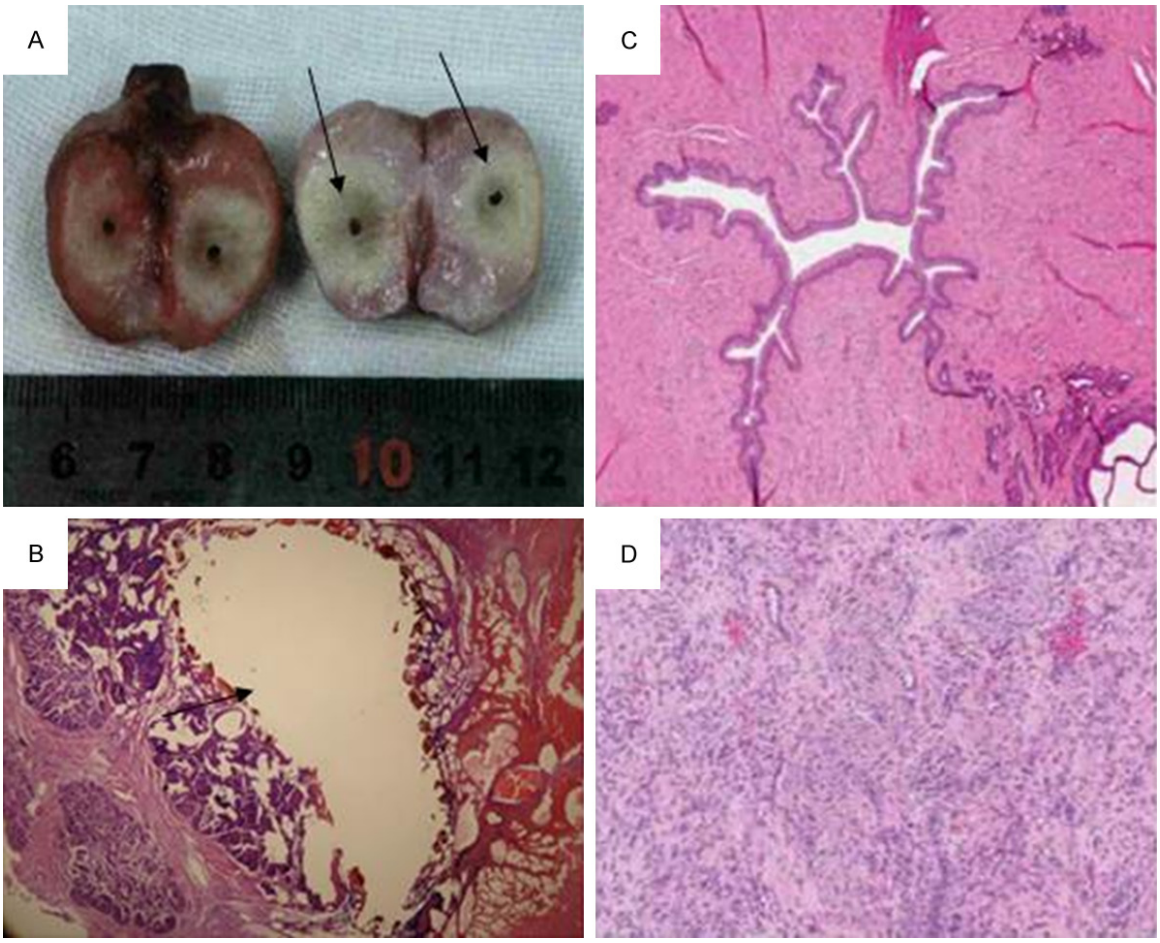

Figure 3. Canine prostate histopathologic examination after bilateral focal Nd: YAG. A: Represents TTC staining of prostate gross cross-sectional slices where there were two distinct vaporizing cavity areas in the ablation zone. As same as appeared in the single focus ablation zone, it apparently presented symmetrically a double of four annular regions in outward hyperemia zone from the center to the margin. B: Focal ablation of prostate after HE staining under pathological expression (*200) which included visible melting stove from the central cavity to bleeding peripheral congestion. C: Represents the abnormal vessel tissues adjacent to the ablation areas. D: Represents the abnormal nervous tissues adjacent to the ablation areas.

t-test and were considered significant when $P<0.05$ (two-tailed).

Results

Imaging evaluation of combination of different power and time of single fiber laser ablation canine prostate

Different power and time of single fiber laser ablation canine prostate were performed in which 24 male dog were evenly separated into two groups. As shown in **Table 1**, the biggest prostate zone size was 6.83±0.34 ml when the parameter was 5 w 5 min, and the second size were 6.63±0.29 ml when it was 5 w 7 min, finally, the smallest size were 4.32±0.62 ml when it was 3 w 5 min. In the Group A, the distinct rising trend existed between 3 w 5 min and 5 w 5 min compared with the descending trend from 5 w 5 min to 7 w 5 min. The similar situation occurred in Group B. There was the apparent ascending trend between 3 w 5 min and 5 w 5 min and the declining trend from 5 w 5 min and 5 w 7 min. Therefore, 5 w 5 min was optimal combination parameter of single focus laser time and power in the study.

Ablation focal boundary of specimen prostate was showed regular oval section in the **Figure 1A**. There was the narrow annular hyperemia edema zone of dark red band surrounding ablation zone. It was apparent that four regions existed in outward area hyperemia from the

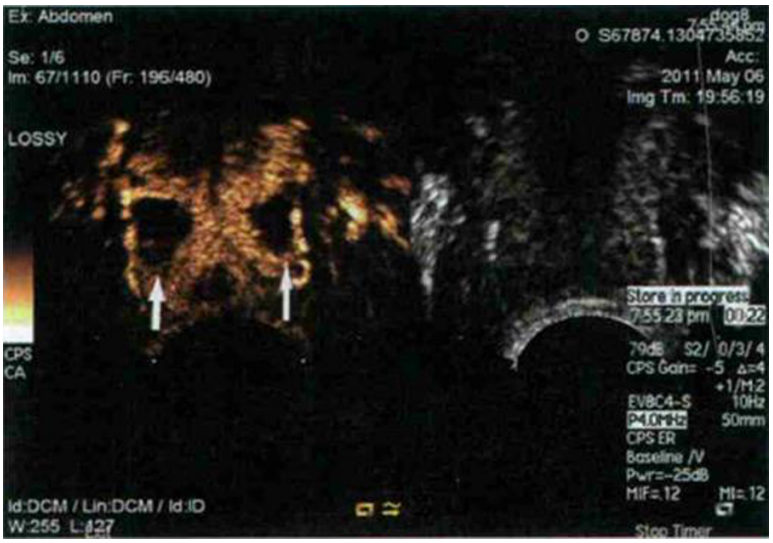

Figure 4. Two-dimensional ultrasonographic examinations of bilateral focus laser ablation. Nearly symmetric micro-bubbles existed in the laser ablation area which was absence of the contract agent, but the surrounding normal prostate tissue filling contrast agent showed clear echogenicity in CEUS examination after 5 min ablation.

center to the margin which was the vaporizing cavity Area, brown carbonized area, dark necrotic area and inflammatory edema area in sequence. The volume of focal ablation was 6.55 cm^3 to 7.48 cm^3, an average of 6.96 cm^3±0.31 cm^3.

As shown in **Figure 1B**, there was large coagulation necrosis area by microscope which was characterized by large evenly dyed red area in the HE staining. In this region, normal glandular structure disappeared and necrosis zone was dotted with bleeding focal point. Moreover, central gasification cavity area and carbonized area both dyed red area in the coagulation necrosis area. The edge of coagulation necrosis, ultimately, was bleeding congestion edema separated with normal glandular structure.

As shown in **Figure 2A** and **2B**, it was obviously that laser ablation process appeared the strong cloudiness echo gradually spreading to the margin in their two-dimensional ultrasonographic examinations before ablation.

As shown in **Figure 2C** and **2D**, there was remarkable micro-bubble in the laser ablation area which was absence of the contract agent, but the surrounding normal prostate tissue filling contrast agent showed clear echogenicity in CEUS examination after 5 min ablation. The coagulation necrosis of ablation area showed the approximate oval area with no contrast agent and strong comparison with the surrounding prostate tissue in which enhancement effect of the contract agent exist, which made their boundary more distinct. The volume of focal ablation was 5.93 cm^3 to 7.83 cm^3, an average of 6.64 cm^3±0.66 cm^3.

Combination of two bilateral focus laser-melting experiment

According to results of single focus ablation examination, 5 min 5 w was chose as one of basic parameters of bilateral focus laser melting experiment. Meanwhile, the ablation zone area of single focus laser melt was 0.7 cm^2 so the superposition of two single needle ablation area, theoretically, was 1.4 cm^2. As shown in **Table 2**, when distance of double needle laser was 3 mm, the ablation area was 1.25 cm^2. With the distance increased, the ablation area significantly extended. The ablation area was 1.53, 1.62, 1.65 cm^2 when focal distance was 6, 9, 12 mm, respectively. Although the area extended to 1.65 cm^2 when the distance enlarged from 9 cm to 12 cm, the extension scale was negligible. Hence, the rational bilateral focal distance was 9 mm.

As shown in **Figure 3A**, there were two distinct vaporizing cavity area in the ablation zone. As same as appeared in the single focus ablation zone, it apparently presented symmetrically a double of four annular regions in outward hyperemia zone from the center to the margin, that is vaporizing cavity Area, brown carbonized area, dark necrotic area and Inflammatory edema area in sequence.

Apparently, more significant coagulation necrosis area by microscope than single focus ablation which was characterized by large evenly dyed red area in the HE staining, as shown in **Figure 3B**. Despite instances of partially occluded capsular arterioles adjacent to the area of ablation, larger arteries and veins or nervous

tissue were not adversely affected by LEDC in the **Figure 3C** and **3D**.

Figure 4 revealed that there were nearly symmetric micro-bubbles in the laser ablation area which was absence of the contract agent, but the surrounding normal prostate tissue filling contrast agent showed clear echogenicity in CEUS examination after 5 min ablation. The coagulation necrosis of ablation area showed the approximate oval area with no contrast agent and strong comparison with the surrounding prostate tissue in which enhancement effect of the contract agent exist, which made their boundary more distinct.

Discussion

Benign prostatic hyperplasia was a common disease among the middle-aged and old males, of which relevant symptom seriously effects on the quality of life of patients. Current drug treatment effect was unsatisfactory, so most patients eventually may need surgery, however the surgical trauma was severe [16]. Moreover, postoperative complications possibly were harmful to the quality of life [17]. Therefore, minimal invasion treatment characterized by safety and validity was still a topic in worth of inquiry [18]. In single needle ablation experiments of our study, changes of melting zone range depend on increase of the power and time. In the Group A, the distinct rising trend existed between 3 w 5 min and 5 w 5 min compared with the descending trend from 5 w 5 min to 7 w 5 min. The similar situation occurred in Group B. There was the apparent ascending trend between 3 w 5 min and 5 w 5 min and the declining trend from 5 w 5 min and 5 w 7 min. Therefore, 5 w 5 min was optimal combination parameter of single focus laser time and power in the study.

Though laser ablation was once applied in the prostate cancer treatment, the usage of laser ablation was decrease gradually because of related small ablation zone [19]. Bilateral optical fibers for the in vitro prostate ablation can be obtained a wide oval, three optical fibers ablation can be obtained a roughly circular structure and four optical fibers ablation can be a square structure [20].

Hence it was feasible to choose multi-fibers therapy program based on lesion size and porous shape or according, which can obtain good conformal therapy effect. No matter when single or bilateral focus ablation, there was remarkable micro-bubble in the laser ablation area which was absence of the contract agent, but the surrounding normal prostate tissue filling contrast agent showed clear echogenicity in CEUS examination after 5 min ablation. The coagulation necrosis of ablation area showed the approximate oval area with no contrast agent and strong comparison with the surrounding prostate tissue in which enhancement effect of the contract agent exist, which made their boundary more distinct.

Disclosure of conflict of interest

None.

Address correspondence to: Bing Hu, Department of Ultrasound in Medicine, Shanghai Jiao Tong University Affiliated Sixth People's Hospital, Shanghai Institute of Ultrasound in Medicine, 600 Yi-Shan Road, Shanghai 200233, China. Tel: +86-21-64369181; E-mail: hubingsh2016@126.com

References

[1] Rubinsky J, Onik G, Mikus P and Rubinsky B. Optimal parameters for the destruction of prostate cancer using Nd: YAG ablation. J Urol 2008; 180: 2668-2674.

[2] Onik G, Mikus P and Rubinsky B. Irreversible electroporation: implications for prostate ablation. Technol Cancer Res Treat 2007; 6: 295-300.

[3] Deodhar A, Monette S and Single GW Jr. Percutaneous Nd: YAG ablation: preliminary results in a porcine model. Cardiovasc Intervent Radiol 2011; 34: 1278-1287.

[4] Thomson KR, Cheung W and Ellis SJ. Investigation of the safety of Nd: YAG ablation in humans. J Vasc Interv Radiol 2011; 22: 611-621.

[5] Bower M, Sherwood L, Li Y and Martin R. Nd: YAG ablation of the pancreas: definitive local therapy without systemic effects. J Surg Oncol 2011; 104: 22-28.

[6] Deodhar A, Monette S, Single GW Jr, Hamilton WC, Thornton R, Maybody M, Coleman JA and Solomon SB. Renal tissue ablation with irreversible electroporation: preliminary results in a porcine model. Urology 2011; 77: 754-760.

[7] Tracy CR, Kabbani W and Cadeddu JA. Nd: YAG ablation: a novel method for renal tissue ablation. BJU Int 2011; 107: 1982-1987.

[8] Miller L, Leor J and Rubinsky B. Cancer cells ablation with Nd: YAG laser. Technol Cancer Res Treat 2005; 4: 699-705.

[9] Schoellnast H, Monette S, Ezell PC, Deodhar A, Maybody M and Erinjeri JP. Acute and subacute effects of irreversible electroporation on nerves: experimental study in a pig model. Int J Med Radiol 2011; 260: 421-427.
[10] Caso JR, Tsivian M, Mouraviev V, Kimura M and Polascik TJ. Complications and postoperative events after cryosurgery for prostate cancer. BJU Int 2012; 109: 840-845.
[11] Onik G, Porterfield B, Rubinsky B and Cohen J. Percutaneous transperineal prostate cryosurgery using transrectal ultrasound guidance: animal model. Urology 1991; 37: 277-281.
[12] Scott W, Cilip C and Fried M. Nd: YAG laser ablation of urinary stones through small-core optical fibers. IEEE J Sel Top Quantum Electron 2009; 15: 435-440.
[13] Spore S, Teichman M, Corbin N, Champion P, Williamson N and Glickman D. Nd: YAG lithotripsy: optimal power settings. J Endourol 2007; 13: 559-566.
[14] White MD, Moran ME, Calvano CJ, Borhan-Manesh A, Mehlhaff BA. Evaluation of retropulsion caused by holmium: YAG laser with various power settings and fibers. J Endourol 1998; 12: 183-6.
[15] Lee H, Ryan T, Teichman J, Kim J, Choi B, Arakeri N and Welch A. Stone retropulsion during Nd: YAG lithotripsy. J Urol 2003; 169: 881-885.
[16] Kang K, Lee H, Teichman J, Oh B, Kim J and Welch J. Dependence of calculus retropulsion on pulse duration during Nd: YAG laser Lithotripsy. Lasers Surg Med 2006; 38: 762-772.
[17] Finley D, Petersen J, Abdelshehid C, Ahlering M, Chou D, Borin J, Eichel L, McDougall E and Cayman K. Effect of Nd: YAG laser pulse width on lithotripsy retropulsion in vitro. J Endourol 2005; 19: 1041-1044.
[18] Marguet J, Sung J, Springhart W, L'Esperance J, Zhou S, Zhong P, Albala P and Preminger D. In vitro comparison of stone retropulsion and fragmentation of the frequency doubled, double pulse Nd: YAG laser and the holmium: YAG laser. J Urol 2011; 173: 1797-1800.
[19] Li W, Fan Q, Ji Z, Qiu X, Li Z. The effects of irreversible electroporation (IRE) on nerves. PLoS One 2011; 6: e18831.
[20] Kalra P, Le NB, Bagley D. Effect of pulse width on object movement in vitro using holmium: YAG laser. J Endourol 2007; 21: 228-31.